The acetaminophen and phenacetin crystals, which are essentially needle shaped, have a tendency to fracture easily and yield weak tablets. Investigations must be conducted with a much wider range of materials.

REFERENCES

(1) E. Shotton and B. Obiorah, *J. Pharm. Pharmacol., Suppl.*, **25**, 37P(1973).

(2) E. Shotton and D. Ganderton, *J. Pharm. Pharmacol.*, **13**, 144T(1961).

(3) K. Ridgway and R. Rupp, *ibid.*, **21**, 30S(1969).

(4) H. Heywood, paper delivered at the Institution of Chemical Engineers Symposium, London, England, Mar. 1969.

(5) E. Shotton and D. Ganderton, *J. Pharm. Pharmacol.*, **12**, 87T(1960a).

(6) *Ibid.*, **12**, 93T(1960b).

(7) W. M. Long, *Powder Metall.*, **6**, 73(1960).

(8) T. Higuchi, T. Shimamoto, S. P. Eriksen, and T. Yakshii, *J. Pharm. Sci.*, **54**, 111(1965).

(9) D. Train and J. A. Hersey, *Powder Metall.*, **6**, 20(1960).

(10) J. N. Carrington, Ph.D. thesis, University of London, London, England, 1958.

(11) J. Versano and L. Lachman, *J. Pharm. Sci.*, **55**, 1128(1966).

(12) S. Leigh, J. E. Carless, and B. W. Burt, *ibid.*, **56**, 888(1967).

ACKNOWLEDGMENTS AND ADDRESSES

Received August 5, 1974, from the *Department of Pharmaceutics, School of Pharmacy, University of London, Brunswick Square, London, WC1N 1AX, England.*

Accepted for publication December 4, 1974.

* Present address: Department of Pharmaceutics, Faculty of Pharmacy, University of Ife, Ile-Ife, Nigeria.

ˣ To whom inquiries should be directed.

Application of Powder Failure Testing Equipment in Assessing Effect of Glidants on Flowability of Cohesive Pharmaceutical Powders

PETER YORK

Abstract □ Powder failure testing equipment was used successfully to study the effect of glidants on the flowability of two cohesive pharmaceutical powders, lactose and calcium hydrogen phosphate, using the flow factor as the flowability parameter. Fine silica, magnesium stearate, and purified talc were investigated as glidants; for each host powder–glidant mixture, an optimum concentration of glidant was observed beyond which no further increase in flowability occurred. The order of efficiency of glidants for both host powders was fine silica > magnesium stearate > purified talc. The mode of action of the three glidants is discussed.

Keyphrases □ Flow properties of cohesive powders—application of powder failure testing equipment (shear cell and tensile tester) □ Glidant—effect on flow factor for powder mixtures, optimum concentration, mode of action □ Powders—effect of glidants on flowability determined using powder failure testing equipment

Over recent years the increasing use of fine powders has emphasized the need for more information regarding their handling and mechanical properties. Fine powders, in general, exhibit nonfree-flowing (*i.e.*, cohesive) properties, which can cause serious problems such as caking of powders in storage and bridging in hoppers. Such problems can lead to the uneven flow of powders and to difficulties in filling operations in various pharmaceutical processes.

To improve the flowability of powders and granulations, a small amount of a second agent, or glidant (1, 2), is often added, usually in powder form. Examples of glidants commonly used in the pharmaceutical industry are talc, magnesium stearate, starch, and fine silica (3). Several postulates have been proposed to explain the mechanism of action of glidants:

1. Removal of electrostatic charges on the surface of the host powder (3, 4).

2. Distribution of glidant through the host powder, and the collection of very fine cohesive host particles onto glidant particle surfaces (5).

3. Selective adsorption of gases and vapors otherwise adsorbed onto the host powders (5).

4. Reduction of van der Waals forces by separation of host powder particles (3).

5. Reduction of interparticular friction and surface rugosity by glidant particles adhering to the surface of the host powder (3, 4).

Several techniques have been employed to study the effects of the addition of glidant to host powders and granulations. Several investigators measured the rate of flow of powder particles from hoppers through circular orifices and measured the flow rate under dynamic conditions (6–8). Other methods have included tablet weight variation (9), vibrating funnel (10), and angle of repose (6, 11, 12). In the latter test, the maximum angle between the surface of a heap of powder and the horizontal plane is measured and values reflect the magnitude of the static coefficient of friction between particles.

All of these tests are most successfully employed for assessing the flowability of relatively coarse powders and granules in the 100–400-μm range (13), and optimum glidant concentrations were derived for particular systems (3, 14). However, the results obtained are significantly affected by the conditions of the test. Angular tests, such as the angle of repose, only provide a qualitative basis for assessing the flow of powders (14). In addition, these techniques do not lend themselves to the study of the flowability of fine cohesive powders, because the measurements become inaccurate (5).

The mechanical properties of cohesive powders can

Table I—Relevant Physicochemical Properties of the Host Powders and Glidants

Property	α-Lactose	Calcium Hydrogen Phosphate	Fine Silica	Magnesium Stearate	Purified Talc
Average particle size, μm	10.10	5.69	0.012[a]	3.61	8.64
Particle density, g/cm³	1.51	2.30	2.20	1.03	2.75
Surface area, m²/g	0.48	0.69	200[a] ± 25	3.65	0.75
Moisture content, % (w/w)	0.04	0.14	0.02	0.08	0.02

[a] Manufacturer's values.

be investigated using powder failure testing equipment (13), *i.e.*, a shear cell and tensile tester, and their flow characteristics can thus be studied in a more scientific and quantitative manner. This investigation was conducted to determine whether this type of equipment can also be employed to study the effect of glidants on the flowability of cohesive pharmaceutical powders and to establish whether optimum glidant concentrations exist for such systems. Clearly, it would be beneficial to be able to select glidants on a scientific basis when they are required to improve the flow properties of cohesive powder formulations.

For comparison, the angle of repose test was also performed using the same powder–glidant mixtures.

EXPERIMENTAL

Materials—The host powders used, α-lactose monohydrate[1] and calcium hydrogen phosphate[2], were reagent grade and were selected as representative cohesive organic and inorganic pharmaceutical powders. The three glidants used were fine silica[3], magnesium stearate[4] BP, and purified talc[5] BP. The relevant physicochemical properties of the powders are listed in Table I.

Average particle sizes were determined using optical microscopy and surface area measurements by an air permeability technique[6], except for fine silica where the particle-size and surface area values in Table I are those quoted by the manufacturer. Particle densities were determined using the specific gravity bottle technique with appropriate immersion fluids.

All powders were dried in thin layers in a hot air oven at appropriate temperatures and were then stored over calcium chloride granules in desiccators.

Preparation of Powder Mixtures—Binary mixtures of lactose containing 0.25, 0.50, 1.0, 2.0, and 4.0% (w/w) of each of the three glidants were prepared by placing the weighed amounts of the powders together in a cylindrical jar and rotating the jar for 20 min to ensure adequate mixing. Similar binary mixtures were prepared to contain calcium hydrogen phosphate and glidant. After mixing, the powder systems were stored over calcium chloride granules in desiccators.

Angle of Repose Measurements—The angle of repose was determined using the funnel method (5). A funnel was positioned centrally over a shallow circular dish of known radius, r, and the powder system was poured evenly through the funnel until the circumference of the dish was touched by the heap of powder. The length of the side of the heap was measured using calipers, h, and the angle of repose, θ, was calculated from the expression $\cos \theta = h/r$. At least five measurements were recorded for the powders and powder mixtures.

Tensile Strength Measurements—The tensile tester was similar to that described by Ashton *et al.* (15); the cell was 9.5 cm (i.d.) and 1.0 cm deep. The mode of operation of the cell was described elsewhere (16), and tensile measurements of the two host powders and the powder–glidant mixtures were made at room temperature. The results for each system were subjected to least-squares regression analysis to enable the tensile strength of any system at a given bulk density to be predicted.

Annular Shear Cell Measurements—An annular-type shear cell was composed of a base, with an annular trough into which the powder was placed, and a close fitting lid containing 18 flights at 20° pitch, the depth of which determined the shear plane level in the powder bed. The inner and outer radii of the annular trough measured 5.6 and 7.6 cm, respectively.

Figure 1 shows a diagram of the cell with a powder sample ready for testing. The base, mounted on a turntable, was rotated at 1 revolution/hr, and the strain-gauge bar was restrained by pins, thus creating a torque in the bar. The developed torque was measured

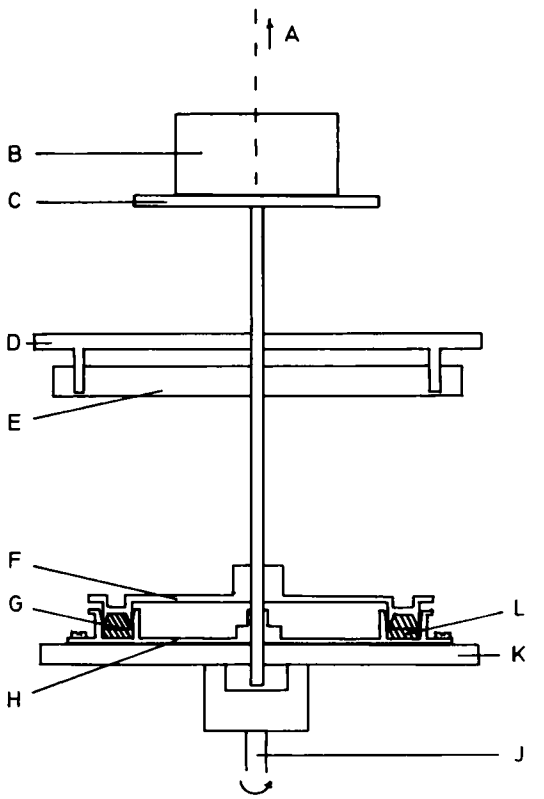

Figure 1—*Diagrammatic representation of annular shear cell with powder bed prepared for testing. Key: A, attachment for counterpoise weight; B, normal load; C, weight platform; D, restraining bar with restraining pins; E, strain-gauge bar; F, shear cell lid; G, flight; H, shear cell base; J, drive shaft (1 revolution/hr); K, platform; and L, powder bed.*

[1] Whey Products Ltd., Crewe, England.
[2] Hopkins and Williams Ltd., Chadwell Heath, Essex, England.
[3] Aerosil 200, De Gussa, Frankfurt, West Germany.
[4] Wilfred Smith Ltd., Edgware, London, England.
[5] Evans Medical Ltd., Speke, Liverpool, England.
[6] Rigden apparatus, Griffin and George Ltd., Wembley, London, England.

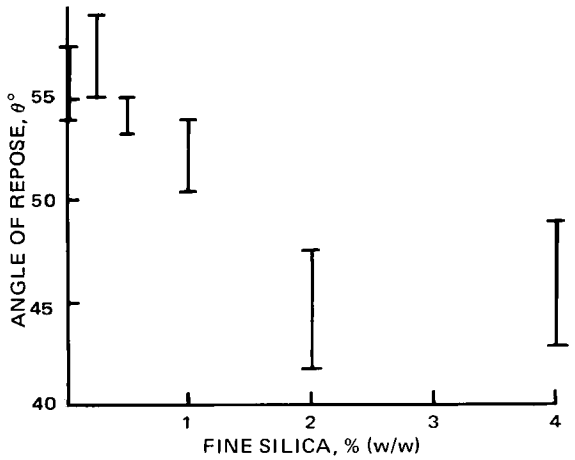

Figure 2—*Representative graph of the angle of repose* versus *the percentage fine silica in lactose–fine silica mixtures. The bar lines represent ±1* SD *from the mean value for each set of data.*

from the output of four silicon semiconductor strain gauges[7] mounted on the bar to form a Wheatstone bridge circuit. Values of shear stress were estimated from the torque developed (17), since the strain gauges had been previously calibrated with known torques using a pulley system.

The bed was prepared by introducing powder in thin even layers into the annular trough in the base and then pressing lightly with an annular disk to ensure a level bed. The lid was then lowered onto the prepared bed, and a normal load was applied using the weight platform. The cell was then rotated with the strain bar restrained. Consolidation of the sample was achieved causing the sample to fail under a normal consolidating load until a steady state, as measured from the output of the strain gauges on a chart recorder, was observed. The lid was then returned manually to its original position, and the sample was sheared under a reduced normal load.

This procedure was repeated after consolidation using different normal loads to obtain a powder yield locus, *i.e.*, a graph of shear stress at failure *versus* normal stress for a given density condition. The failure stress under steady-state conditions for the consolidating normal load was taken to represent the end-point of the locus. Results were only used if the height of the bed did not differ by more than ±2% from the original value, and the bulk density of the sample was calculated from the weight and volume of the sample. Four yield loci were obtained for each powder system by using four different consolidating loads.

The annular-type shear cell has certain advantages over the cylindrical type (18) in that smaller quantities of powder are required (50–80 g) and measurements can be made in a much shorter time. However, the annular cell suffers from the fact that at any particular angular deflection, powder at the outer wall of the cell's annulus is strained more than that at the inner wall so there is a small variation in shear stress across the width of the sample. For this investigation, this effect was minimized by making the annular width small and by employing a low rate of shear (1 revolution/hr).

RESULTS AND DISCUSSION

The angle of repose is not a fundamental property of a powder, since the value obtained partly depends upon the technique of measurement (13). For a static heap of powder, the angle of repose has a limiting value. Particles in the surface layer of the heap exist in an equilibrium situation, with the gravitational force balanced by interparticular attractive and frictional forces. Any particle that lies above this layer will slide down the heap since the gravitational force will predominate (5).

[7] Strain-gauge types 2A-1A-120P and 2A-1A-120N, Ether Ltd., Stevenage, England.

Table II—Powder Flow Classification by Flow Factor (18)

Flow Factor	Powder Flow Classification
>10	Free flowing
4—10	Easy flowing
1.6—4	Cohesive
<1.6	Very cohesive

Representative results of angle of repose measurements are illustrated in Fig. 2 for the lactose–fine silica mixtures, and the graph shows a general decrease in the angle of repose with increasing glidant concentration. Significant scatter of results can be observed due to such factors as the nonuniformity of heap and the formation of a steep-sided peak at the end of the test resulting in a concave surface. Similar scatter of results was observed for the other host powder–glidant mixtures in the study. This type of angular test thus appears to be generally unsatisfactory for any accurate assessment of the flowability of cohesive powder–glidant mixtures.

Powder failure tests, however, provide an alternative approach. Of the several flowability parameters that can be derived from the results of failure tests, *e.g.*, cohesion (4), angle of internal friction (19), and index of flow (19, 20), it is essential to select the most relevant factor. Since the problems related to the gravity flow of cohesive powders, *e.g.*, flow from hoppers and flow into dies, reduce the efficiency of many pharmaceutical processes, for the present investigation the flow factor (F.F.) (18) was used to assess flowability. Increasing values of the flow factor indicate that a powder or powder mixture is becoming more free flowing under the effect of gravity (18) (Table II).

To obtain the flow factor from a powder yield locus, the tensile strength value was calculated at the bulk density of the locus (Fig. 3) and then data from each locus were analyzed by regression analysis, using the logarithmic form of the Warren Spring Laboratory yield locus equation (20):

$$\log \tau = K + \frac{1}{n} \log(\sigma + T) \qquad \text{(Eq. 1)}$$

$$K = \log \frac{C}{T^{1/n}} \qquad \text{(Eq. 2)}$$

where:

σ = normal stress (grams per square centimeter)
τ = shear stress at failure (grams per square centimeter)
C = cohesion (grams per square centimeter)
T = tensile strength (grams per square centimeter)
n = index of flow

Flow factors were then obtained using the locus equations by estimating f_c (unconfined yield stress) and σ_{max} (maximum normal stress) for each locus (18) (Fig. 3). These stresses are derived by drawing two Mohr semicircles tangential to the yield locus, one passing through the origin and intersecting the abscissa at f_c and the second passing through the end-point of the locus and giving σ_{max}. A computer program was written to carry out this analysis. The flow factor is then defined as the reciprocal of the slope of graphs of f_c *versus* σ_{max} for a number of loci obtained for an individual powder or mixture. In this present investigation, these graphs have a curvature, as illustrated in Fig. 4, and the flow factor

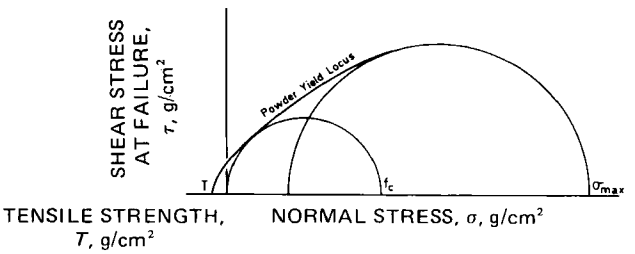

Figure 3—*Diagram illustrating the derivation of the unconfined yield stress,* f_c, *and maximum normal stress,* σ_{max}, *from a powder yield locus.*

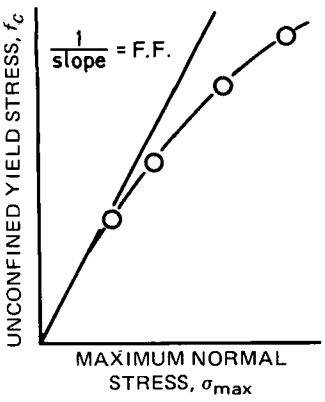

Figure 4—*Diagram illustrating the derivation of the flow factor (F.F.) from a graph of the unconfined yield stress,* f_c, versus *the maximum normal stress,* σ_{max}.

is determined as the reciprocal of the slope of the tangent to the graph at the origin (18).

Graphs of the flow factor *versus* the percentage (w/w) glidant in the mixtures with both lactose and calcium hydrogen phosphate are shown in Figs. 5, 6, and 7 for fine silica, magnesium stearate, and purified talc, respectively. The largest changes in the flow factor are produced by the addition of fine silica, with increases from 1.9 to 10.4 for lactose and from 3.9 to 10.5 for calcium hydrogen phosphate. Both increases represent a change in classification from cohesive to free flowing according to Table I. The optimum concentrations of fine silica, estimated from Fig. 5, were 0.85% (w/w) for lactose and 1.45% (w/w) for calcium hydrogen phosphate. Addition of further glidant to the host powder beyond these concentrations produced no additional increase in flow factor.

It has been proposed that the mechanism whereby fine silica operates to improve flowability is adherence to the surface of host powder particles (14). Approximate calculations of the concentration of glidant required to form an adsorbed layer one particle thick can be made, using the surface area measurement of the host powder and the average particle size of the glidant, assuming that the glidant particles are spherical and uniformly closely packed over the surface of the host powder. Such estimates are in close agreement with the optimum percentage concentration of fine silica as found by experiment (Table III), and this finding seems to support the proposed mechanism of action. If the fine silica particles were adsorbed onto host powder particles, a smoothing out of the host particle surfaces would take place, thus decreasing both friction and mechanical interlocking of particles during flow. In addition, the host–host interactions at particle contact points would be replaced by weaker glidant–glidant forces.

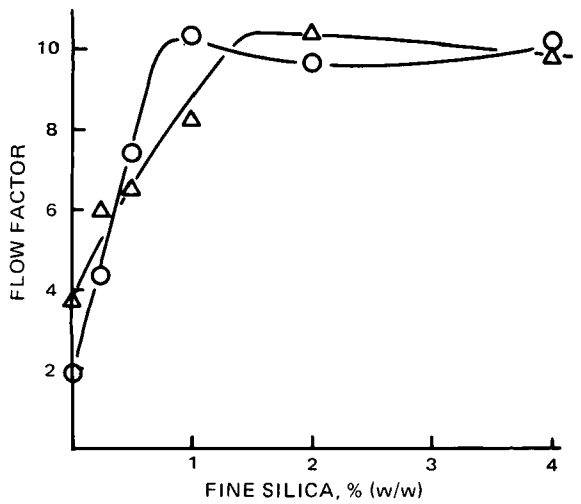

Figure 5—*Graphs of changes in the flow factor of host powder–fine silica mixtures at different concentrations of fine silica. Key:* ○, *lactose–fine silica mixtures; and* △, *calcium hydrogen phosphate–fine silica mixtures.*

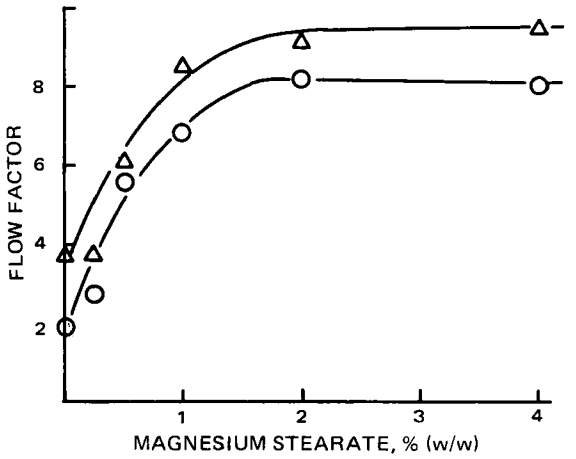

Figure 6—*Graphs of changes in the flow factor of host powder–magnesium stearate mixtures at different concentrations of magnesium stearate. Key:* ○, *lactose–magnesium stearate mixtures; and* △, *calcium hydrogen phosphate–magnesium stearate mixtures.*

Table III—Optimum Glidant Concentrations

	Optimum Glidant Concentration, % (w/w)			
	Fine Silica		Magnesium Stearate,	Purified
Host Powder	Experimental	Theoretical	Experimental	Talc, Experimental
α-Lactose	0.85	0.96	1.75	2.25
Calcium hydrogen phosphate	1.45	1.38	2.20	2.45

Magnesium stearate and purified talc do not produce such large increases in the flow factor as does the fine silica (Figs. 6 and 7), although the former glidant does improve the flowability of both lactose and calcium hydrogen phosphate from cohesive to easy flowing (Table II). In all cases, an optimum percentage glidant concentration can be estimated (Table III). Magnesium stearate, unlike fine silica, is hydrophobic and appears to function as a glidant by accumulating in voids between hydrophilic host particles (14), thereby reducing interparticular friction and attractive forces between host particles. To achieve a significant improvement in the flowability of cohesive powders, a larger percentage of magnesium stearate is required compared with fine silica, since the optimum concentrations of magnesium stearate are 1.75% (w/w) for lactose and 2.20% (w/w) for calcium hydrogen phosphate.

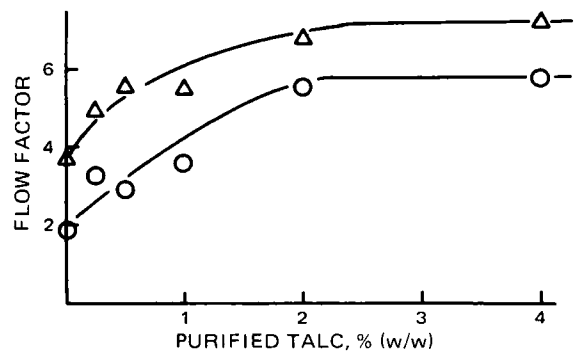

Figure 7—*Graphs of changes in the flow factor of host powder–purified talc mixtures at different concentrations of purified talc. Key:* ○, *lactose–purified talc mixtures; and* △, *calcium hydrogen phosphate–purified talc mixtures.*

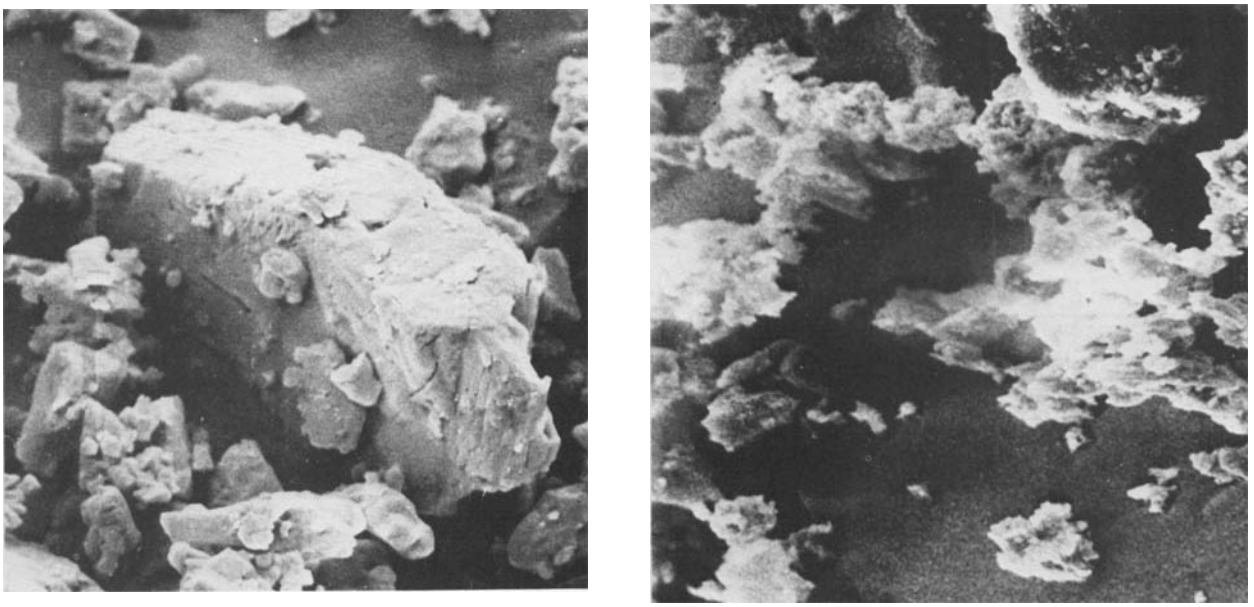

A B

Figure 8—*Electron scanning microscope photographs of host powder particles. Key: A, α-lactose (about 6500×); and B, calcium hydrogen phosphate (about 3250×).*

Figure 7 indicates that purified talc is the least effective of the three glidants studied, both in terms of the increase in the flow factor and in requiring the largest concentrations to achieve maximum improvement in flowability. Indeed, the increases in the flow factor do not appear to be sufficient to impart free-flowing properties to either of the host powders.

A possible mode of action for purified talc has been proposed in terms of its laminar crystalline structure which, when subjected to the low shearing forces created when powders flow, rolls up into a spherical structure (21). The presence of such spheres would then improve the flowability of the host powder.

The differences in optimum percentage concentration obtained for the three glidants with both host powders can be attributed to differences in the mechanism of action of the glidants, the physical and chemical nature of the materials, and the relative particle sizes of the host and glidant particles. Indeed, it is conceivable that if purified talc had an average particle size similar to that of the fine silica, it might also function by adsorbing to form a monoparticular layer over the host powder, thereby improving its efficiency as a glidant.

Higher values of optimum glidant concentration were derived for calcium hydrogen phosphate than for lactose with all three glidants studied. This finding can be explained not only by the larger surface area per gram of the calcium hydrogen phosphate but also by the different surface structure of the two powders (Fig. 8).

Electron scanning microscope photographs reveal that the lactose particles have a relatively smooth and angular structure, while calcium hydrogen phosphate particles possess a more convoluted and rougher surface. Thus, calcium hydrogen phosphate would be expected to require the presence of relatively more glidant particles to improve its flowability.

From this discussion, it is evident that powder failure testing equipment can be successfully used to assess the efficiency of glidants in improving the flowability of cohesive powders and also to select optimum glidant concentrations. This kind of equipment could be usefully employed in pharmaceutical formulation in cases where cohesive powders and mixtures cause powder flow problems.

SUMMARY

1. The angle of repose test was unsuitable for assessing the flowability of cohesive lactose and calcium hydrogen phosphate powders and their mixtures with glidants.

2. Powder failure testing equipment, *i.e.*, annular shear cell and tensile tester, were successfully employed to study the effects of three glidants (fine silica, magnesium stearate, and purified talc) on the flowability of cohesive lactose and calcium hydrogen phosphate powders. Flowability was assessed using the flow factor parameter.

3. For both host powders, the order of efficiency in increasing the flow factor was in the order fine silica > magnesium stearate > purified talc.

4. In all systems, optimum glidant concentrations were observed. For the same glidant, these values were higher for calcium hydrogen phosphate than for lactose; this finding is attributed to differences in the surface area and structure of the two powders.

REFERENCES

(1) W. A. Strickland, *Drug Cosmet. Ind.*, **85,** 318(1959).

(2) K. Munzel and W. Kagi, *Pharm. Acta Helv.*, **29,** 53(1954).

(3) T. M. Jones, Symposium on Powders, Society of Cosmetic Chemists of Great Britain, Dublin, Ireland, Apr. 1969.

(4) M. Peleg and C. H. Mannheim, *Powder Technol.*, **7,** 45(1972).

(5) B. S. Neumann, in "Advances in Pharmaceutical Sciences," vol. 2, Academic Press, London, England, 1967, pp. 194, 207.

(6) G. Gold, R. N. Duvall, B. T. Palermo, and J. G. Slater, *J. Pharm. Sci.*, **55,** 1291(1966).

(7) *Ibid.*, **57,** 667(1968).

(8) T. M. Jones and N. Pilpel, *J. Pharm. Pharmacol.*, **18,** 429(1966).

(9) L. L. Augsburger and R. F. Shangraw, *J. Pharm. Sci.*, **55,** 418(1966).

(10) O. Leoveanu, N. Zaharia, and V. Pilea, *Rev. Chim.*, **17,** 112(1966).

(11) E. Nelson, *J. Amer. Pharm. Ass., Sci. Ed.*, **44,** 435(1955).

(12) D. J. Craik and B. F. Miller, *J. Pharm. Pharmacol.*, **10,** 136T(1958).

(13) N. Pilpel, in "Advances in Pharmaceutical Sciences," vol. 3, Academic Press, London, England, 1971, pp. 174–176.

(14) N. Pilpel, *Mfg. Chem. Aerosol News*, **Apr. 1970,** 19.

(15) M. D. Ashton, R. Farley, and F. H. H. Valentin, *J. Sci. Instrum.*, **41,** 763(1964).

(16) P. York and N. Pilpel, *J. Pharm. Pharmacol.*, **24,**

47P(1972).
(17) J. F. Carr and D. M. Walker, *Powder Technol.*, 1, 369(1967).
(18) A. W. Jenike, "Gravity Flow of Solids," Bull. 108, Utah Engineering Experimental Station, University of Utah, Salt Lake City, Utah, 1961.
(19) J. C. Williams and A. H. Birks, *Powder Technol.*, 1, 199(1967).
(20) M. D. Ashton, D. C.-H. Cheng, and F. H. H. Valentin, *Rheol. Acta*, 4, 206(1966).
(21) D. Train and J. A. Hersey, *J. Pharm. Pharmacol.*, 12, 97T(1960).

ACKNOWLEDGMENTS AND ADDRESSES

Received August 26, 1974, from the *Department of Pharmaceutics, Faculty of Pharmacy, University of Khartoum, Khartoum, Sudan.*

Accepted for publication December 5, 1974.

The author gratefully acknowledges the facilities provided by Dr. N. Pilpel at Chelsea College, University of London, for carrying out this work and also the assistance of Mr. B. Nicholls, Computer Centre, University of Khartoum, in the writing of the computer programs. Thanks are also due to Mr. Weinberg of Chelsea College for the electron scanning microscopy work.

Rapid, Sensitive Colorimetric Method for Determination of Ethinyl Estradiol

MOHAMED A. ELDAWY ˣ, A. S. TAWFIK*, and S. R. ELSHABOURI

Abstract □ A colorimetric procedure, based on the formation of an azo dye by condensation of diazotized 5-chloro-2,4-dinitroaniline with ethinyl estradiol, was developed. An alkaline solution of ethinyl estradiol is reacted with the reagent, and the resulting color is measured at 450 nm. Absorbance *versus* concentration is linear up to 10 μg/ml; the lower limit of detection is 1 μg/ml under the conditions studied. Replicate analysis showed good agreement, and an average recovery of 99.6 ± 0.3% was obtained for analyses of synthetic mixtures. Vitamins and minerals likely to be present along with ethinyl estradiol in certain geriatric formulations, as well as ordinary tablet excipients and coating materials, do not interfere with the precision of the method or development of the color. The method is applicable to progestin–estrogen preparations. Assay results on various single-component as well as contraceptive commercial samples are reported.

Keyphrases □ Ethinyl estradiol in progestin–estrogen and vitamin/mineral geriatric preparations—colorimetric analysis □ Progestin–estrogen contraceptive tablets—colorimetric analysis of ethinyl estradiol □ Geriatric formulations containing vitamins, minerals, and estrogens—colorimetric analysis of ethinyl estradiol □ Colorimetry—analysis, ethinyl estradiol in progestin–estrogen and vitamin/mineral geriatric preparations

Several methods for the analysis of ethinyl estradiol are available in the literature, including UV (1), GLC after suitable derivatization (2, 3), and colorimetric methods (4–8). The USP XVIII colorimetric procedure (9), which is a modification of the Kober reaction (4), suffers from several disadvantages exhibited by the rather limited solubility of ethinyl estradiol in isooctane. These disadvantages might be circumvented by using an isooctane–chloroform mixture instead as modified in the first supplement to USP XVIII. The Kober reaction, in spite of many modifications (10–12), is time consuming, and the color development is critically dependent upon reagent composition, reaction time, and temperature. Interference by other nonphenolic steroids also can occur (13).

The suitability of diazotized 4-amino-6-chloro-*m*-benzenedisulfonamide for the determination of a number of estrogens has been investigated (14). The method, although suitable for routine analysis, has rather low sensitivity. The lower limit of detection is 0.05 mg of estrogen/ml of sample solution. Commercially available dosage forms, especially geriatric formulations, are usually of very low dosage (0.008–0.05 mg/tablet or capsule). Consequently, the sensitivity of this procedure is such that single-tablet analysis of most commercial dosage forms is not feasible.

In spite of its high sensitivity, the Liebermann–Burchard reaction-based fluorometric method of James (15), with 0.5 μg/ml as a lower limit for detection, is not applicable to progestin–estrogen preparations. Progestational steroids produce a color in the Liebermann–Burchard reaction that quenches the fluorescence of ethinyl estradiol.

It has been observed in these laboratories that diazotized 5-chloro-2,4-dinitroaniline couples with phenolic compounds to form products with extremely stable colors; this finding offers the basis for a rapid and sensitive method for the determination of pharmaceuticals containing a phenolic hydroxy group (16). The suitability of this reagent for the determination of ethinyl estradiol was investigated, and a rapid and sensitive colorimetric method for the determination of ethinyl estradiol was developed. This method eliminates the disadvantages of the Urbanyi and James methods, as well as those of the Kober reaction.

EXPERIMENTAL[1]

5-Chloro-2,4-dinitroaniline—This compound was prepared by a reported procedure (17). Several crystallizations from ethanol yielded an analytical sample, mp 174°.

Reagents and Solutions—The following were used: 5-chloro-2,4-dinitroaniline (0.2% ethanolic solution), sodium nitrite (3% aqueous solution), 1 *N* hydrochloric acid, 2 *N* sodium acetate, 0.1 and 1 *N* sodium hydroxide, and absolute ethanol.

[1] A Hungarian-made Spektromom 203 spectrophotometer was used.